PII: S0032-3861(98)00053-6

Polymer Vol. 39 No. 20, pp. 4707–4714, 1998

0032-3861/98/$19.00+0.00

Morphology of liquid crystalline epoxy composite matrices based on the diglycidyl ether of 4,4′-dihydroxy-α-methylstilbene

H.-J. Sue[a,*], J. D. Earls[b], R. E. Hefner Jr[b], M. I. Villarreal[b], E. I. Garcia-Meitin[b], P. C. Yang[b], C. M. Cheatham[b] and C. J. G. Plummer[c]

[a]*Department of Mechanical Engineering, Texas A & M University, College Station, TX 77843-3123, USA*

[b]*The Dow Chemical Company, Freeport, TX 77541, USA*

[c]*Laboratoire de Polymères, Département des Matériaux, Ecole Polytechnique Fédérale de Lausanne, Lausanne CH-1015, Switzerland*

(Received 27 October 1997; revised 16 December 1997; accepted 16 December 1997)

The morphologies of various diglycidyl ethers of 4,4′-dihydroxy-α-methylstilbene-based liquid crystalline epoxy (LCE) formulations have been studied as matrices for high performance composites. Reflected light optical microscopy, selected area electron diffraction, micro-Raman spectroscopy and transmission electron microscopy of thin sections and replicas of etched surfaces were employed to probe both the micrometer-scale and nanometer-scale LCE morphology in infusion moulded, uni-weave graphite fibre composites. The results suggest that various sizes and shapes of LCE domains can be formed in the matrix resin, depending on the cure schedule and the LCE curative composition. Preferred molecular orientation along the graphite fibres can be achieved if the LCE resin is cured so as to promote extensive linear chain extension, thus giving a high concentration of mesogenic segments. Approaches for aligning mesogenic segments in the composite are discussed as well as the potential benefits of doing so.

(Keywords: liquid crystalline epoxy resin; composite; molecular orientation)

INTRODUCTION

Liquid crystalline polymers (LCPs) are known to exhibit many desirable physical and mechanical properties, such as outstanding barrier properties, high fracture toughness, extremely high moduli when oriented, high heat-deflection temperatures, low moisture absorption, and unusual optical, electrical, and thermal properties[1–6]. These properties cannot be readily obtained from conventional amorphous or semi-crystalline polymers. At present, only thermoplastic LCPs, such as Vectra®, are commercially available. Unfortunately, these thermoplastic LCPs are quite expensive, require high processing temperatures and exhibit poor mechanical properties transverse to the orientation direction[5,7]. They are only utilized in small volume, highly specialized applications.

Recent development of thermoset LC epoxies (LCE) based on the diglycidyl ether of 4,4′-dihydroxy-α-methylstilbene (DGE-DHAMS) has indicated great potential for producing a new line of high performance and low cost products for aerospace, electronic, infrastructure and sporting goods applications[1–4]. The synthesis, chemistry, key physical and mechanical properties, and potential applications of the DGE-DHAMS-based liquid crystalline epoxy (LCE) resin systems have been reported in the literature[1–4]. The morphologies of these DGE-DHAMS-based neat epoxies, i.e., without the presence of fibres, have also been shown to be strongly dependent on the mesogen content and the curing schedule[1,2]. In general, these LCEs possess extremely high tensile moduli and strength when molecularly oriented, high fracture toughness, high ductility, outstanding chemical and solvent resistance, high *Tg*, low water absorption, and ease of processing suitable for high performance composite applications.

For reference, the chemical structure of the DGE-DHAMS is given below,

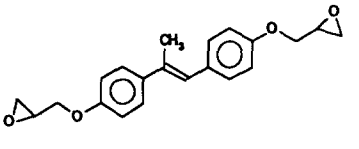

DGE-DHAMS

where the *para*-disubstituted α-methylstilbene moiety forms the rod-like mesogenic core. The double bond on the DGE-DHAMS backbone is found to be quite stable with no observable thermal degradation detectable up to 300°C[5,8]. The liquid crystallinity begins to develop upon chain extension resulting from reaction of the DGE-DHAMS segments with appropriate curing agents at temperatures above the monomer melting point of 135°C.

It is well known that so-called transcrystalline growth of crystals in semi-crystalline polymers can occur at the surface of certain substrates, such as graphite fibres[9–11]. It therefore seems possible that preferred LC domain growth along the graphite fibre surface can also occur on chain extension and crosslinking of the DGE-DHAMS monomers. The present work is an investigation of the feasibility of preparing molecularly aligned LCEs as the matrix in

* To whom correspondence should be addressed

graphite fibre composites prepared via an infusion moulding process. It is speculated that if the LCE can be molecularly aligned in composite systems, greatly improved stiffness, toughness, damage tolerance, and compressive strength can be achieved. The potential benefits of using molecularly aligned LCE composites for high performance structural applications are discussed.

EXPERIMENTAL

Materials

To study how the curing conditions and composition affect the morphology in LCE composites, three LCE formulations were chosen for composite morphology studies. These LCE systems are (1) DGE-DHAMS:sulfanilamide (1:1 ratio by equivalent weight (E.W.)) [LCE-1], (2) DGE-DHAMS:DHAMS:sulfanilamide: catalyst (1:0.4:0.6:0.002 ratio by E.W.) [LCE-2], (3) DGE-DHAMS: TACTIX* 556 epoxy resin:sulfanilamide (0.79:0.21:1.0 ratio by E.W.) [LCE-3].

MI1610 uni-weave graphite fibre (6K G30-500), woven by Mutual Industries (Philadelphia, PA), was used in making the LCE composite laminates. The laminates were prepared via an infusion moulding process. The areal density of this uni-weave fabric was 250 g cm^{-2}. The composite laminates were fabricated using a unidirectional $[0^\circ]_{18}$ lay-up, and were about 3.5 mm thick. The composition and curing schedule for the LCE composites are given below:

LCE Composite System I [LCEC-1]:
Matrix: LCE-1
Curing Schedule: 4 h @ 120°C + 1 h @ 140°C + 1 h @ 160°C + 1 h @ 180°C + 1 h @ 200°C + 2 h @ 230°C

LCE Composite System II [LCEC-2]:
Matrix: LCE-2
Curing Schedule: 4 h @ 120°C + 1 h @ 140°C + 1 h @ 160°C + 1 h @ 180°C + 2 h @ 200°C

LCE Composite System III [LCEC-3]:
Matrix: LCE-2
Curing Schedule: 4 h @ 150°C + 1 h @ 175°C + 2 h @ 200°C

LCE Composite System IV [LCEC-4]:
Matrix: LCE-3
Curing Schedule: 4 h @ 120°C + 1 h @ 140°C + 1 h @ 160°C + 1 h @ 180°C + 1 h @ 200°C + 2 h @ 230°C

The curing schedule and composition in these resins were chosen based on an earlier finding[1,2], which investigated the influences of curing schedule and composition on morphology, toughness, modulus, and flow behaviour of a variety of LCE resins, to give either a high level of liquid crystallinity (LCE-1), a tough matrix (LCE-2), or an easily processable high glass-transition temperature matrix (LCE-3) for LCE composites.

Microscopic investigation

Reflected light optical microscopy. The LC domain morphology in LCE composites was examined using reflected light optical microscopy (ROM). The interior of the composite laminate was exposed by cutting the composite sample using a diamond saw at the mid-plane either perpendicular or parallel to the fibre direction. The interior LCE composite surfaces were polished to a 0.3 μm finish using an alumina powder suspension for ROM investigation. The polished composite surfaces were then studied using an Olympus Vanox-S optical microscope under bright field and cross polarization conditions.

Etching/replication. In order to determine the appropriate etching time and etching solution concentration, four LCEC-1 composite samples were polished near the core using a Leco rotary water polisher until a 0.3 μm finish was achieved on the sample surface. A permanganic acid etching solution was prepared by adding 20 mL of deionized water to a 500 mL Erlenmeyer flask in an ice-bath with a stirring bar. While stirring, 20 mL of concentrated phosphoric acid was slowly added to the mixture followed by 10 mL of concentrated sulfuric acid. The solution was carefully monitored to prevent overheating. Finally, 0.25 g potassium permanganate was slowly added to the mixture.

Three of the polished samples were placed in glass jar containing the etching solution and immersed for different times (30 min, 60 min, and 75 min) at 60°C. The samples were rinsed in a wash solution for 2 min immediately after etching. The wash solution was prepared by adding 20 mL of concentrated sulfuric acid to 70 mL of deionized water. After removing the samples from the wash solution, the samples were rinsed in a 10% hydrogen peroxide solution, and then in deionized water.

Examination of the blocks using reflected Nomarski interference contrast on an Olympus Vanox research microscope revealed that an etching time of 75 min gave the best structural contrast for the LCE domain features, which showed only indistinct contrast in polished unetched control samples.

The etched surface was replicated for transmission electron microscopy (TEM). Polyvinyl acetate (PVA; 2 g) was slowly dissolved in 20 mL filtered deionized water heated to 60°C. For replication, one drop of the PVA solution was placed on the etched surface of the sample and allowed to dry overnight. Once dried, the PVA film was carefully peeled away from the sample and placed face-up on a glass slide. The ends of the film were secured to the slide with tape to prevent curling, and it was shadowed with carbon/platinum at a 30° angle of incidence in an Edwards Vacuum evaporator. Regions of interest in the shadowed PVA film were cut into rectangular sections slightly smaller than the diameter of a TEM grid. These were floated onto the surface of filtered deionized water at 80°C to dissolve the PVA film. The remaining carbon/platinum replica was picked up using a slotted grid and placed on a 100-mesh formvar-coated TEM grid. The replicas were examined using a Jeol 2000FX TEM at an accelerating voltage of 100 kV.

Selected area electron diffraction and direct TEM imaging. To investigate molecular organization in the matrix, bulk samples were sectioned at room temperature using a Reichert–Jung Ultracut E ultramicrotome and a Diatome 45° diamond knife, to give 40–50 nm thick films. These were picked up on 400 mesh TEM grids covered with an ultra-thin carbon film. Selected area electron diffraction (SAED) was performed on both the Jeol 2000FX TEM and a Philips EM 430 TEM, at accelerating voltages of 200 and 300 kV, respectively, and with various camera lengths. Both aluminium and sodium-beta-alumina were used as standards. The aluminium was prepared by evaporation of the metal onto a formvar-coated grid. International centre for Diffraction Data (ICDD) standard 4-787 was used as the reference for the Al diffraction peaks.

* Trademark of the Dow Chemical Company

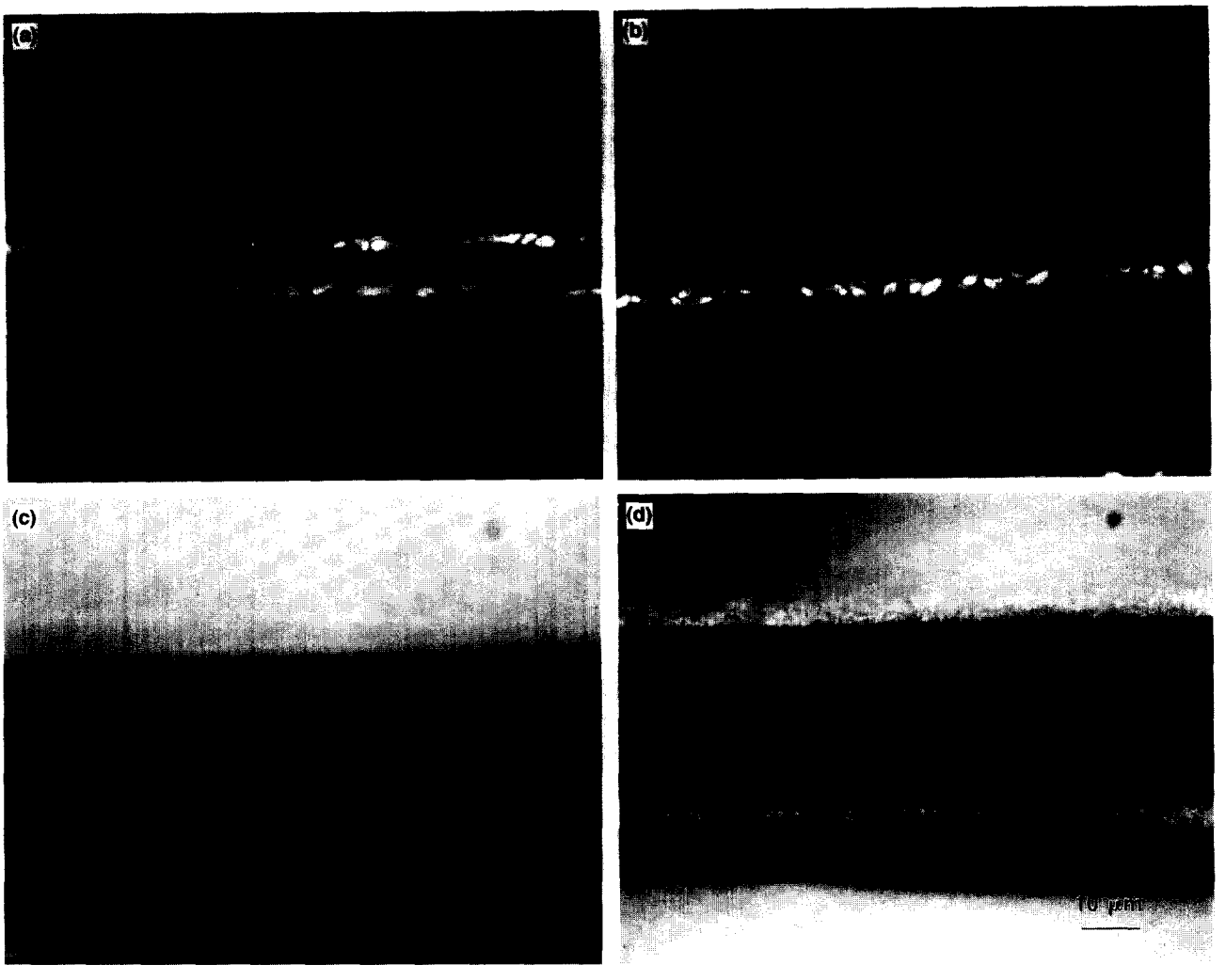

Figure 1 ROM of LCE composites under crossed-polars. a) LCEC-1, b) LCEC-2, c) LCEC-3, and d) LCEC-4. It is evident that the formation of LC domains vary among the LCE composites prepared. The arrows indicate the resin-rich regions

For direct imaging, use was made of a Philips EM 430 at 300 kV (point-to-point resolution 2.3 Å), aligned with the aid of gold nanoclusters deposited on an ultrathin carbon film. Suitable regions of the LCE sample were identified in diffraction mode using a very low beam intensity. A low-dose unit was employed to limit subsequent exposure of the area of interest to the time necessary to record the image, focusing being carried out on an adjacent region of the sample at the final magnification. Rapid sample degradation (as reflected by the fading of the SAED diffraction peaks)limited the range of magnifications which could be used. This could partly be compensated by underexposing the films (Kodak SO-163) and using increased developing times (15 min in full strength Kodak developer D-19). Nevertheless, in spite of these precautions, maximum magnifications were restricted to about 45 000 × .

Micro-Raman spectroscopy. A Dilor confocal triple spectrograph was operated with the first two stages used as a subtractive double to acquire the Raman spectra. A 3-stage Peltier cooled CCD detector was mounted in the focal plane of the third stage. An argon ion laser tuned to 514.5 nm was used for excitation of the sample, with approximately 0.2 mW measured at the sample. The 100 × objective employed for these studies allowed a spatial resolution of 1–2 μm. This spatial resolution is sufficient for a local LC domain size of 5–10 μm in the interlaminar region of the LCEC-1 composite. The Raman spectra were obtained with an integration time of 200 s. Orientation in the liquid crystalline epoxy between carbon fibres was determined by collecting polarized Raman scattering both parallel and perpendicular to the carbon fibres.

The Raman intensities of peaks at 1600 and 1200 cm^{-1} were utilized to monitor the molecular orientation. The peak at 1600 cm^{-1} is an aromatic ring peak. The assignment of the 1200 cm^{-1} peak is believed to be related to the polymer backbone.

RESULTS AND DISCUSSION

The main objective of this research is to learn how the morphologies of LCE matrices develop in graphite fibre composite systems. The mechanical properties of the LCE composites, which are in turn affected by the morphology in the composite, will be reported separately[12].

Reflected light optical microscopy

ROM was used to characterize the overall LC domain size and shape in each sample. As shown in *Figure 1*, four different LC morphologies were observed for the four LCE composites evaluated. Extended domains spanning the interlaminar regions were seen in LCEC-1 (*Figure 1*a), more randomly oriented, cigar-shaped LC domains were seen in LCEC-2 (*Figure 1*b) and there was no sign of LC domain formation in LCEC-3 (*Figure 1*c). In the case of LCEC-4, only sub-micrometer, randomly oriented LC

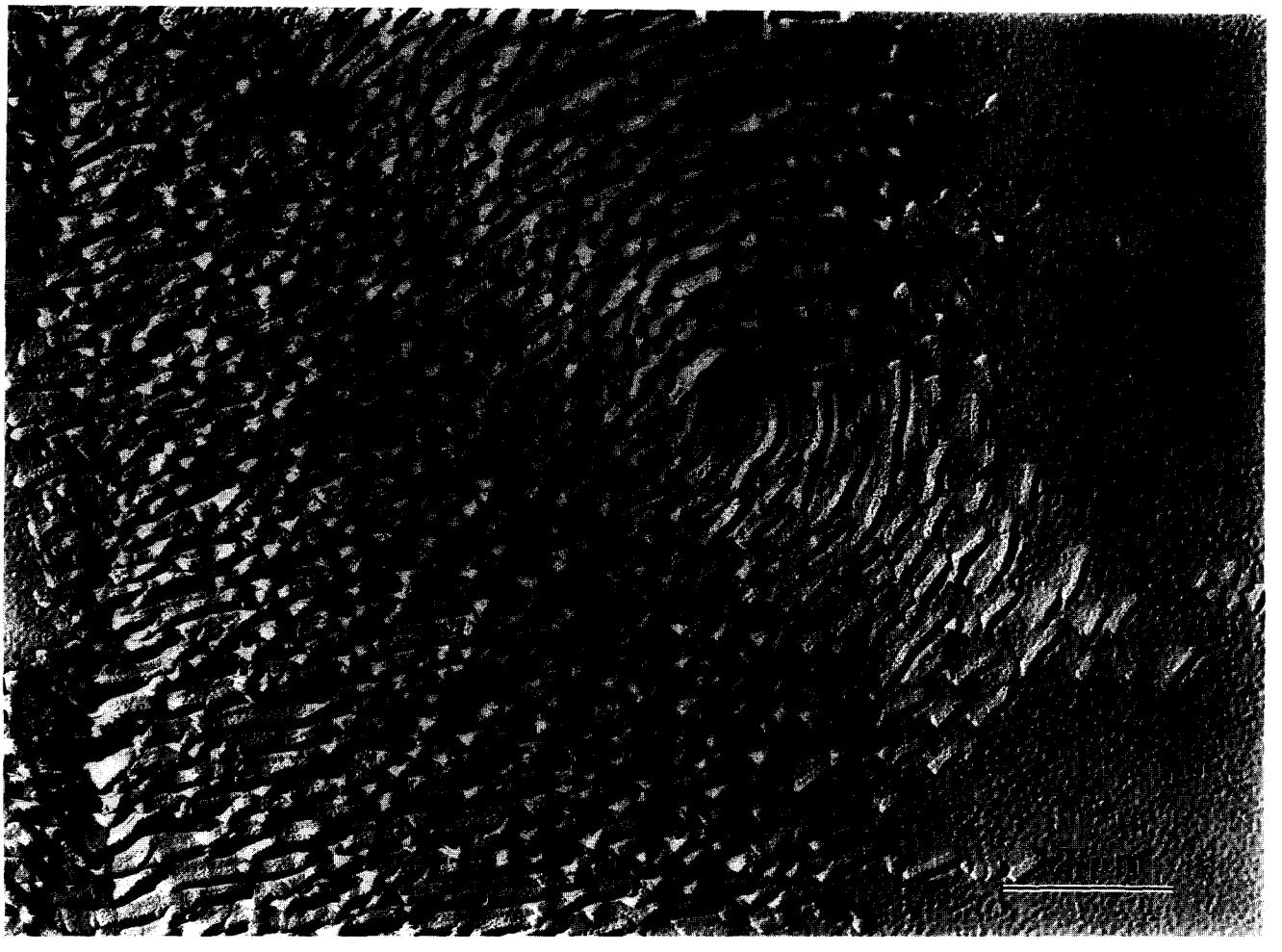

Figure 2 TEM etching/replication micrograph of LCE-1 sample. The spirally arranged LC domain can be readily seen

domains could be detected in the interlaminar regions (*Figure 1*d), which contrasted with the highly organized texture of LCEC-1. The reason LCEC-3 contained no LC domains was that the matrix (LCE-2) was cured at 150°C, which is above the isotropic curing temperature (140°C) for LCE-2. Since only LCEC-1 showed signs of long range molecular alignment, this composite was chosen for more thorough morphological investigation, to be described in the following sections.

The above findings suggest that the curing schedule, the monomer(s) and the curing agent(s) can greatly affect the resulting LC morphology in LCE composites. Therefore, it is imperative that one clearly identify the morphology in different LCE composites when comparisons of the physical and mechanical properties are to be made.

It was observed that when the LC domains were large, the density and modulus of the LCEs were significantly higher than in LCEs containing small or no LC domains. This implies that the well-aligned LC domains may help resist buckling of graphite fibres, which would in turn greatly improve the compressive strength of the composites. This is highly desirable for structural applications in the aerospace industry.

It was further observed that when the LCEC-1 composite was viewed in the plane perpendicular to the fibre direction, the LC domains showed no apparent birefringence. This suggests either random organization of the mesogenic α-methylstilbene rigid-rods, or homeotropic alignment parallel to the fibre direction. Moreover, observation of substantial birefringence in sections taken parallel to the fibre direction (*Figure 1*a) confirmed the presence of significant orientation of the rigid rods along the fibre direction. This conclusion was further supported by the experimental results to be described as follows.

Etching and replication

To verify the utility of the etching and replication technique, a LCE-1 bulk sample, cured using the same conditions as the LCEC-1 composite, was investigated. It was expected that the less well-organized amorphous phase or the bi-phase regions of the LCE-1 matrix would be etched away relatively rapidly, so that the well-aligned mesogenic domains would remain as salient features. This would lead to a 'ridge-and-valley feature' surface topography.

Figure 2 shows the morphology within a single large LC domain in LCE-1. The spiral pattern seen in the figure in this case indicated the formation of the LC domain to involve nucleation and growth, which is consistent with the findings of Lin et al.[5]. Thus, the etching and replication technique appears to be quite effective for LCE systems. Moreover it is noteworthy that the morphology of the LC domain was significantly different from the multilamellar morphologies typically encountered in etched spherulites in conventional semi-crystalline polymers[13].

To investigate the detailed features of the LCE matrix in the resin-rich regions of the LCEC-1 composite, use was again made of the etching and replication technique. As shown in *Figure 3*, there appeared to be a molecularly ordered structure within such regions, showing alignment with respect to the graphite fibre. The repeat distance in this

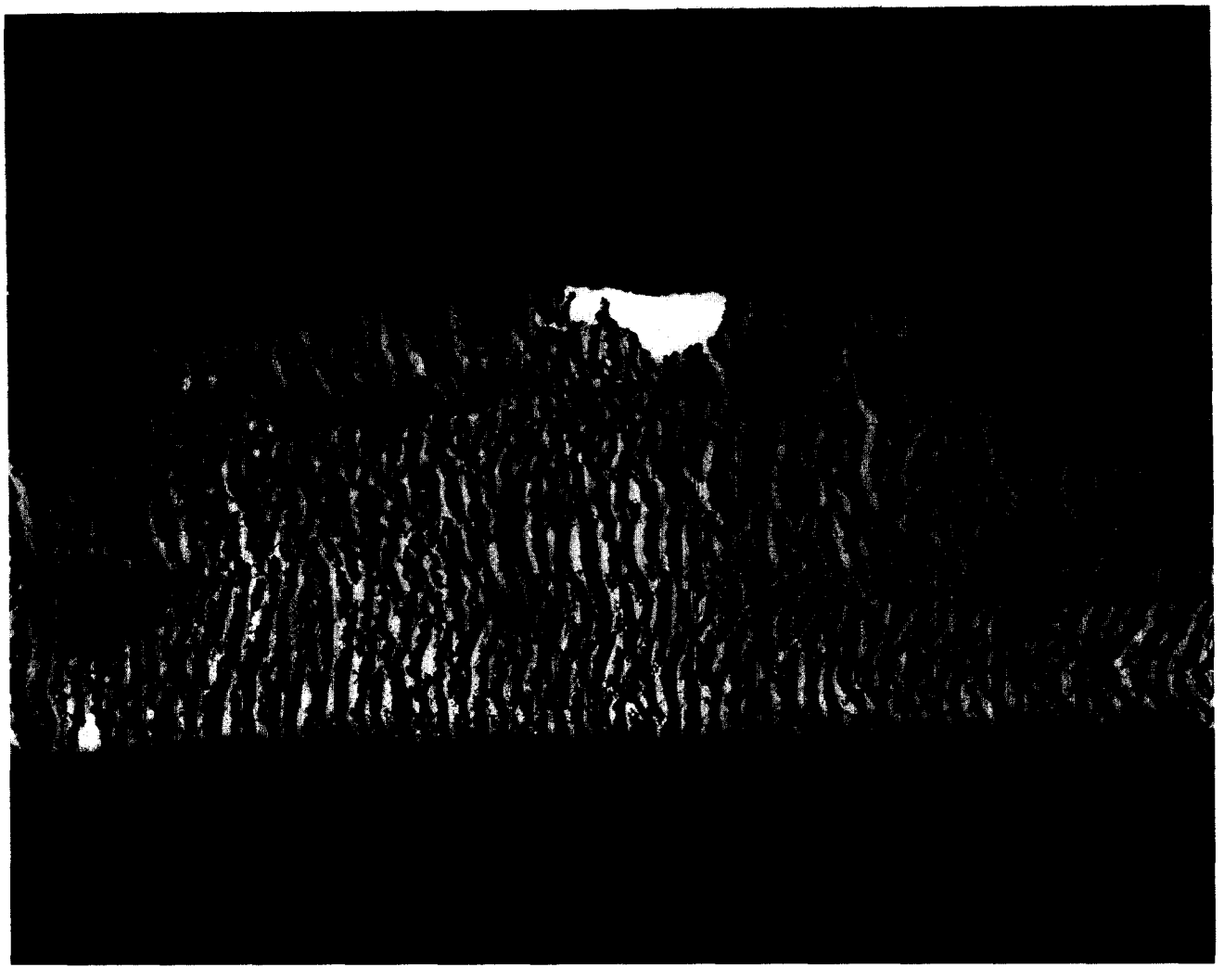

Figure 3 TEM etching/replication micrograph of LCEC-1 composite sample. It is evident that well-organized mesogenic rigid rods are present between the graphite fibres

structure was approximately 200 nm. Although it is not clear how the molecules organize based on this information alone, it seems certain that ordered mesogenic segments are present in the LCEC-1 composite. However, since this is, to our knowledge, the first attempt to apply the etching and replication technique to morphological investigations of liquid crystalline epoxies, care has to be taken in interpreting the above findings.

In order to investigate further the molecular organization responsible for the etched textures, direct TEM and SAED observations were therefore made of thin sections from the bulk polymer.

Selected area electron diffraction and direct tem imaging

There has been widespread use of TEM and SAED for polymer structure characterization, although their success often depends on the quality of the samples[14,15]. In the present case, ultrathin sectioning was relatively straightforward and the large domains observed optically were easily identifiable in bright-field images such as shown in *Figure 4*a (the intervening material showed far more limited long-range orientation). *Figure 4*b shows a corresponding SAED pattern taken from within a suitably oriented domain, showing a diffuse, arced equatorial scattering peak corresponding to a spacing of about 4.7 Å, and a diffuse meridional peak corresponding to a spacing of about 1.9 Å. These are typical of aligned LC polymers. However, in addition to these diffuse peaks, a very sharp meridional reflection was observed corresponding to a spacing of 21.0 Å, along with second and third order peaks (the existence of a characteristic spacing of 21.0 Å in this material is confirmed by small angle X-ray scattering). The structure is thus clearly smectic, with the mesogenic units forming layers, with their molecular axis roughly perpendicular to the plane of the layer, consistent with results from previous X-ray scattering work[5].

To observe the overall organization of these layers within the domains, bright field phase contrast images were obtained from regions showing strong low angle meridional scattering at $1/21.0\ \text{Å}^{-1}$. High resolution phase contrast images taken under Scherzer and extended Scherzer conditions apparently contained little structural information. In order to enhance the contrast of features with characteristic spacings, d, in the 20 Å range, the underfocus, Δf, was therefore calculated from

$$\Delta f = d^2/2\lambda$$

where $\lambda = 0.0196$ Å is the wavelength of the electron beam[16], giving in this case $\Delta f \sim 1\ \mu$m. *Figure 5*a shows a detail of 21.0 Å fringes from part of a single LC domain imaged under these conditions and *Figure 5*b shows an overview of the same domain at lower magnification. Since the fringes are unlikely to be visible in the final

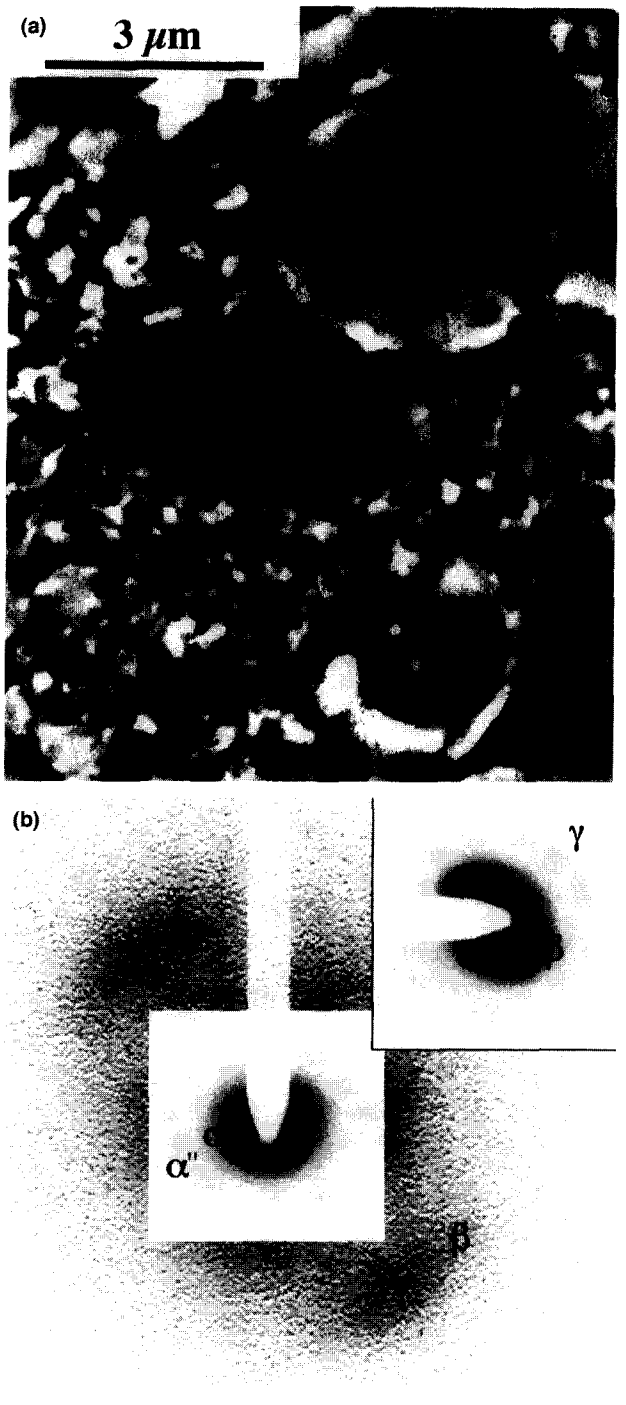

Figure 4 (a) A low magnification bright field TEM image of domains in a thin section of LCEC-1 (the arrow indicates the cutting direction); (b) the corresponding SAED pattern shown at two different camera lengths. The peaks labelled α, β and γ correspond to d-spacings of 21, 4.7 and 1.9 Å respectively, α' is the second order peak corresponding to α

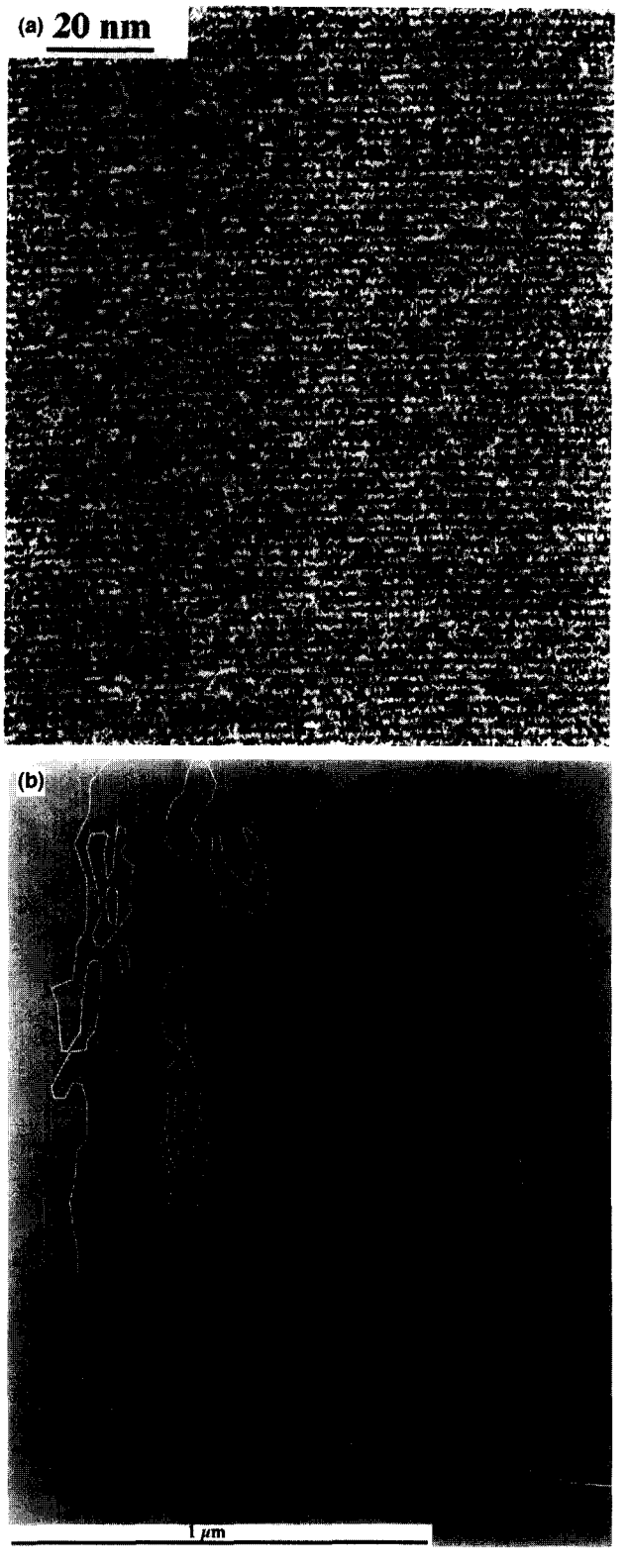

Figure 5 (a) Part of a TEM phase contrast image showing fringes with 21 Å spacing; (b) overview of the domain from which (a) was taken and in which the regions containing coherent fringes, and the fringe orientation (dark lines) have been shown schematically

reproduction of *Figure 5*b, the regions over which they are continuous have been outlined, and the local orientation indicated. Continuous fringes extended over areas comparable with that of the whole domain (typical total domain widths were between 2 and 5 μm), suggesting a remarkable degree of organization. Nevertheless, as may be seen from both *Figure 5*a and *Figure 5*b, there is slight curvature of the fringe trajectories, although in this case it does not appear systematic (we have not so far been able to obtain phase contrast images of the spiral texture shown in *Figure 2*). It should be emphasized that mesogens themselves are oriented normal to the fringes in *Figure 5*, and that these latter correspond to smectic layers, rather than superpositions of individual molecules. There was some suggestion of systematic fluctuations in the fringe contrast along their length, so that the domains were subdivided into ribbon-shaped regions of high contrast fringes extending perpendicular to the fringe direction (cf. *Figure 5*b. where a few elongated regions showing no fringes at all were observed within the main domain, toward the left-hand

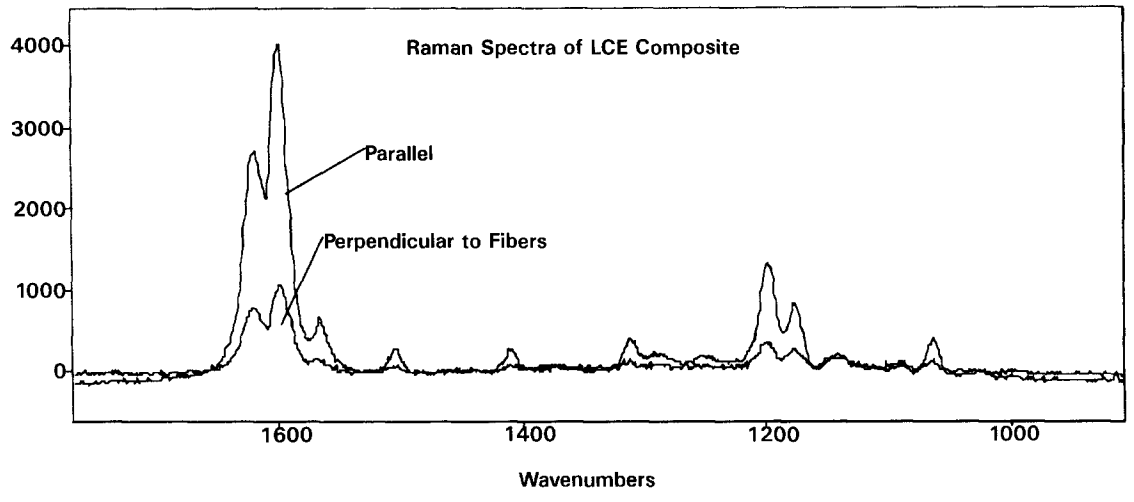

Figure 6 Micro-Raman spectrum of LCEC-1 composite sample. Preferential orientation of mesogenic segments along the fibre direction is observed

side of the image). This has not been quantified since the morphology of the ribbons was not well defined and there was concern over the possibility of artifacts. Moreover the coherence of the fringes was maintained between adjacent ribbons. However if these contrast fluctuations represent variations in local order, this may explain the coarse ridged topography of the etched domains (less ordered regions etching more rapidly than the surrounding material).

Micro-Raman spectroscopy

The micro-Raman technique was utilized to probe further the orientation of the mesogenic units with respect to the fibre direction in the composites. The spectra obtained for LCEC-1 are shown in *Figure 6*. The Raman peak at 1600 cm^{-1} is an aromatic ring peak. The assignment of the 1200 cm^{-1} peak is believed to be related to the polymer backbone. From *Figure 6*, it is evident that the Raman intensity along the fibre direction is much stronger than that perpendicular to the fibre direction. Therefore, these results, although not absolutely conclusive, again suggest that the smectic, mesogenic segments of DGE-DHAMS are mostly aligned along the fibre direction.

If the substrate-induced molecular alignment is not sufficient to generate LC formation or it takes too long to induce molecular orientation under ordinary curing conditions, it should be possible to apply either an electric or magnetic field to further promote LC alignment during the composite consolidation process[3–18]. It is conceivable that full scale commercial composite panels with controlled molecular orientation can be made using the LCE resins investigated in this study.

Based on the above findings, the proposed LCE orientation is modelled in *Figure 7*. The rigid rod-like mesogenic segments should be aligned along the graphite fibre direction. The thickness of the well-aligned LC domains extends approximately 5 μm away from the fibre surface. Beyond that, signs of misalignment begin to occur (*Figure 2*). Defects can also be observed at the junction of the two outward-growing LC domains. Preliminary investigation of impact damage mechanisms suggests that cracks grow randomly in the interlaminar regions, instead of following the orientation of the LC domain or at the junction between the two LC domain fronts[12]. This suggests that the LCE matrix is fundamentally different from thermoplastic liquid crystalline polymers in that the strength and toughness along the lateral direction of the LCE are relatively good. This again indicates the value of potential LCEs for structural composite applications.

It is evident that, based on the present work and the research work conducted by others on non-LCE systems[19–21], it is possible to control the morphology of the LCE matrix in graphite fibre composites. Therefore, superior environmental degradation resistance and significantly improved high temperature modulus retention of the composite should be available. The compressive strength of the composite should be greatly increased due to the high stiffness of the LCE matrix. Furthermore, it is possible that the fracture resistance of the LCE composite in the crack propagation direction, which is parallel to the molecular orientation, is higher than that for thermoplastic LC composites due to the crosslinking of the mesogenic segments. This crosslinking for the oriented bulk LCE has been observed to provide transverse properties similar to a conventional epoxy resin[17].

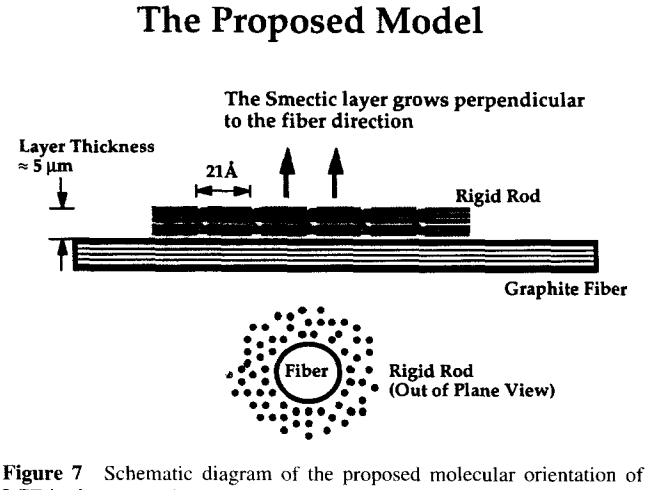

Figure 7 Schematic diagram of the proposed molecular orientation of LCE in the composite

CONCLUSION

The morphology of LCE composites based on DGE-DHAMS have been studied using ROM, TEM, SAED, X-Ray diffraction, and micro-Raman techniques. Evidence of mesogen alignment along the graphite fibre direction is found for a slowly cured LCE resin. It is possible that LCEs may be utilized to substantially boost thermoset performance for electronic and aerospace structural composite applications.

ACKNOWLEDGEMENTS

The authors would like to acknowledge Anne Leugers of Dow Chemical who performed the micro-Raman analysis. For the TEM work, the assistance of C.C. Garrison and the Interdepartmental centre for Electron Microscopy of the EPFL is greatly appreciated.

REFERENCES

1. Sue, H.-J., Earls, J. D. and Hefner, R. E. Jr., *J. Mater. Sci.*, 1997, **32**, 4031.
2. Sue, H.-J., Earls, J. D. and Hefner, R. E. Jr., *J. Mater. Sci.*, 1997, **32**, 4039.
3. Earls, J. D., Hefner, R. E. Jr., and Puckett, P. M., US Patent No. 5463091, 1995.
4. Earls, J. D., Hefner, R. E. Jr., and Puckett, P. M., US Patent No. 5218062, 1993.
5. Lin, Q., Ph.D. Thesis, University of Michigan, Ann Arbour, MI, 1994.
6. Barclay, G. C., Ober, C. K. Pa, Papathomas, K. I. and Wang, D. W., *J. Polym. Sci., Part A: Polym. Chem.*, 1992, **30**, 1831.
7. Donald, A. M. and Windle, A. H. *Liquid Crystalline Polymers*. Cambridge University Press, Cambridge, UK, 1992.
8. Earls, J. D. and Hefner, R. E. Jr., personal communication, 1994.
9. Petermann, J., Cai, Y. and Wittich, H., *J. Appl. Polym. Sci.*, 1997, **65**, 67.
10. Ishida, H., Neyman, G. and Lando, J. B., *Compos. Interfaces*, 1995, **2**, 351.
11. Incardona, S., Migliaresi, C., Wagner, H. D., Gilbert, A. H. and Marom, G., *Composites Sci. Techn.*, 1993, **47**, 43.
12. Sue, H.-J., Yang, P. C., Earls, J. D. and Hefner, R. E. Jr., to be published.
13. Schultz, J. *Polymer Materials Science*. Prentice Hall, New Jersey, 1974.
14. Martin, D. C. and Thomas, E. L., *Polymer*, 1995, **36**, 1743.
15. Lovinger, A. J., Lotz, B., Davis, D. D. and Padden, F. J. Jr., *Macromolecules*, 1993, **26**, 3494.
16. Pradere, P. and Thomas, E. L., *Macromolecules*, 1990, **23**, 4954.
17. Smith, M. E., Benicewicz, B. C., Douglas, E. P., Earls, J. D. J.D and Priester, R. D., *Polym. Preprints*, 1996, **37**, 50.
18. Langlois, D. A., Smith, M. E., Benicewicz, B. C. and Douglas, E. P., PMSE, 74, American Chemical Society, 1996, 135.
19. Adams, P. M. and Mallon, J. J., *Mol. Cryst. Liq. Cryst.*, 1991, **208**, 65.
20. Bhama, S. and Stupp, S. I., *Polym. Eng. Sci.*, 1990, **30**, 228.
21. Chapoy, L. L. *Recent Advances in Liquid Crystalline Polymers*. Elsevier Applied Science, New York, 1985.